

High-temperature, classical, real-time dynamics of non-abelian gauge theories as seen by a computer

J. Ambjørn^a, K.N. Anagnostopoulos^b and A. Krasnitz^c

^a The Niels Bohr Institute, University of Copenhagen,
Blegdamsvej 17, DK-2100 Copenhagen Ø, Denmark.
E-mail: ambjorn@nbi.dk

^b Department of Physics, University of Crete,
P.O. Box 2208, GR-71003 Heraklion, Greece.
E-mail: konstant@physics.uoc.gr

^c CENTRA and Faculdade de Ciências e Tecnologia,
Universidade do Algarve,
Campus de Gambelas, P-8000, Faro, Portugal.
E-mail: krasnitz@ualg.pt

Abstract

We test at the electroweak scale the recently proposed elaborate theoretical scenario for real-time dynamics of non-abelian gauge theories at high temperature. We see no sign of the predicted behavior. This indicates that perturbative concepts like color conductivity and Landau damping might be irrelevant at temperatures corresponding to the electroweak scale.

PACS: 11.15.Ha, 12.38.Mh, 05.20.Gg, 05.40.+j.

Keywords: sphalerons; baryon asymmetry; lattice simulations; magnetic mass.

1 Introduction

The study of $SU(2)$ gauge theories at high temperatures is important for our understanding of the electroweak theory in the early universe. One effect which has been of interest in this context is the baryon-number non-conservation in the electroweak theory, caused by the anomaly of the baryonic current. After the work of Kuzmin, Rubakov and Shaposhnikov [1] it was realized that the baryon number non-conservation, caused by thermal field fluctuations between gauge-equivalent vacua with different winding numbers, could be large in the unbroken phase of the electroweak theory. A quantitative verification of the KRS-scenario requires non-perturbative real time simulations of hot thermal gauge theories, a task we still do not know how to perform from first principles. However, following suggestions by [2] that one could use *classical* thermal gauge theory to address the question, it was shown in [3] that transitions between vacua with different winding numbers is unsuppressed at high temperatures in the unbroken phase of the electroweak theory. Starting with [4, 5], much work has since gone into refining the numerical techniques used and turning the qualitative statements into quantitative measurements [6, 7, 8, 9, 10, 11, 12] and also in understanding to what extent the notion of topology used in the continuum anomaly calculations is still valid in the lattice simulations [13].

In order to address the determination of the rate of “sphaleron” transitions quantitatively one needs either to understand the corrections to the rate induced by using classical thermodynamics rather than the correct quantum field theory thermodynamics, or to develop better non-perturbative methods suited for real time simulations. The latter alternative is of course preferable since it might allow us to address many other non-perturbative questions which involve real-time dynamics of non-abelian gauge theories at high temperatures, by correctly incorporating thermal fluctuations in the ultraviolet.

Much progress has been made in this direction over the last decade, starting with the concept of hard thermal loops, and culminating with the effective small-momentum, low-frequency theory of Bödeker [14] and its interpretation in terms of color conductivity [15, 16]. In ordinary (abelian) plasma physics low frequency magnetic fields decay slower than naively expected due to Landau damping. It is now understood that the same mechanism applies to a pure non-abelian plasma, where the hard, high frequency modes couple to the low frequency magnetic modes much like the charged particles in an abelian plasma, and in this way produce a new time scale for the magnetic fluctuations. While the dominant long-range magnetic fluctuations will occur at the (non-perturbative) length scale of the order $1/g^2T$, the lifetime of the fluctuations will be of the order $\omega \sim g^4T \ln(1/g)$.

On a more quantitative level the soft classical fields (momentum $k \leq gT$) couples to hard currents according to

$$\dot{\mathbf{E}} = \mathbf{D} \times \mathbf{B} - \mathbf{J}_{\text{hard}}, \quad (1)$$

where

$$\mathbf{J}_{\text{hard}} = \sigma \mathbf{E} + \boldsymbol{\xi}, \quad (2)$$

and where the effective noise term $\boldsymbol{\xi}$ is determined by the fluctuation-dissipation theorem:

$$\langle \xi_i^a(t, \mathbf{x}) \xi_j^b(t', \mathbf{x}') \rangle = 2T \sigma \delta_{ij} \delta^{ab} \delta(t - t') \delta(\mathbf{x} - \mathbf{x}'). \quad (3)$$

In (1) σ denotes the so-called color conductivity, which to a leading log approximation is given by

$$\sigma = \frac{m^2}{\gamma}, \quad m^2 = \frac{2}{3} (gT)^2, \quad \gamma = \frac{3}{16\pi} g^2 T \ln(1/g). \quad (4)$$

m denotes the Debye screening mass and γ the hard gauge fields damping rate (given here for pure $SU(2)$ gauge theory). The derivation of (1) is valid in a frequency range

$$\omega \ll k\gamma \quad \text{and} \quad k \geq g^2 T. \quad (5)$$

Strictly speaking, in order for (5) to be valid, one has formally to require that $\ln 1/g$ be parametrically large. In this frequency range one can ignore the time derivative in (1). Then

$$\mathbf{D} \times \mathbf{B} = \sigma \mathbf{E} + \boldsymbol{\xi}. \quad (6)$$

Working in temporal gauge *and ignoring non-linearities*, one obtains from (6)

$$k^2 \mathbf{A} + \sigma \dot{\mathbf{A}} = \boldsymbol{\xi}, \quad (7)$$

which leads to the decay of gauge correlators:

$$\langle \mathbf{A}(t) \mathbf{A}(0) \rangle \propto \exp \left\{ - \frac{k^2}{\sigma} t \right\}. \quad (8)$$

The decay time τ for $k \sim g^2 T$ is thus of the order

$$\tau \sim \frac{1}{g^4 T \ln(1/g)}, \quad (9)$$

i.e., much longer than the non-perturbative length scale $1/(g^2 T)$.

While this picture no doubt gives an appropriate description of the long wavelength, low frequency thermal fluctuations for spatial scales up to $1/(g^2 T)$ and time scales up to $1/(g^4 T \ln(1/g))$ when $\ln(1/g)$ in some sense can be considered large, the question arises how well it describes “sphaleron” physics at the electroweak scale where $\alpha \approx 1/30$, *i.e.* $g \approx 0.65$.

Presently there are good indications that the picture works well at the above value of g . Real time computer simulations have been done, using various ways of implementing the hard currents [6, 8, 10] The primary observable in the simulations has been the sphaleron rate. This is so for good reasons. Firstly, it is an important observable which might play a role in explaining the baryon asymmetry of the

universe. Secondly, it is believed to be dominated by long wavelength, classical thermal field fluctuations, *i.e.*, one can hope that the classical theory, or at least the improvements, like Bödeker’s effective field theory, will allow us to determine this (non-perturbative) rate by computer simulations. Until now all computer simulations basically agree, and there is a kind of consensus in the community that the sphaleron rate goes as predicted by Arnold, Son and Yaffe (ASY) and Bödeker.

The purpose of this article is not to cast doubt on the effective theory of Bödeker and ASY, but only to point out that it is may not be clear that it can be applied to the electroweak theory for temperatures around the phase transition. The derivation of the effective theory, in particular in the framework of ASY, uses perturbative concepts like real time gauge correlators and color conductivity, and the explicit behavior of these objects as functions of momentum k and frequency ω are used. While some of these objects are gauge dependent they can nevertheless be measured in the same computer simulations used to determine the sphaleron rate and one can directly check if their long wavelength, low frequency part show the behavior predicted by the effective theory. If not, one could be tempted to conclude that one needs to go to higher temperature, and that one should *not* try to match the sphaleron rate to formulas based on the validity of the long wavelength, low frequency effective theory.

The rest of this paper is organized as follows: in Section 2 we describe shortly our simulation setup and the set of gauge-covariant and gauge-invariant objects likely to be governed by a long wavelength effective theory. Our results are reported in Section 3. Section 4 concludes.

2 Simulation setup and observables

As mentioned in the Introduction, there presently exists no genuine non-perturbative way of simulating real-time processes in non-abelian gauge theories from first principles. Solving the classical field equations of motion is as close as one can get to a study from first principles, in the sense that no external parameters are introduced into the system. The caveat is, of course, that the classical thermal distribution is incorrect: while the thermal fluctuations in the quantum theory are cut off at scale T , the thermal fluctuation of the classical theory is only cut off at the cut-off scale $\Lambda \sim 1/a$, where a is the lattice spacing. The non-perturbative, long-distance magnetic sector of the thermal theory is not expected to be very sensitive to an exact location of the ultraviolet cutoff, as long as the cutoff is not too close to the magnetic scale. At the same time, the perturbative sector will be changed and, whenever one encounters the Debye mass one has to make a replacement:

$$m_D^2 \sim g^2 T^2 \rightarrow g^2 T/a. \quad (10)$$

A typical high-temperature field configuration will be dominated by its large-momentum components, *i.e.*, for the classical field theory the components of the

order of the cut off, for the full quantum theory the components of order T . If one is interested in the dynamic behavior of the system at large distances (from the magnetic screening length and above) one needs a way to filter out the prevalent large-momentum components of the field. One way to do so is by cooling. In the context of sphaleron transitions the method was first applied in the very first numerical work on the sphaleron transitions at the electroweak phase transition, [17], as well as in the study of the flow of eigenvalues of the Dirac operator in presence of lattice sphalerons [13]. Later it was introduced as a tool to reduce the large momentum, short distance lattice artifacts of the sphalerons in real time simulations [9]. As discussed in [9], moderate cooling is best suited for this purpose, since it leads to an exponential decay of high-frequency modes. In this way the sphaleron profile, buried in the thermal fluctuations, will be enhanced. However, one can go a step further and simply view the cooling as a general procedure for integrating out the large momentum components of the thermal classical field theory, basically leaving us with the large distance physics of the classical theory.

Our procedure is thus the following: first we generate a thermal field configuration for an $SU(2)$ classical Yang-Mills theory on a lattice [5], for a given temperature T . We then let the system evolve according to the classical equations of motion. At selected instances along the classical trajectory we extract long-wavelength information from the field configuration by cooling (we defer to the next section the discussion of how deep the cooling should be). Using the new configurations we can measure whatever observables we have in mind, and since we are probing the low momentum, classical sector of the theory, we should be able to compare our results with the prediction from effective theory given by (1)-(2) provided we make the appropriate substitutions like (10) and provided that we are in a coupling constant and temperature region where (1) and (2) are valid.

The classical Hamiltonian dynamics is most conveniently studied in the temporal gauge where the electric field $\mathbf{E}(\mathbf{x}, t)$ is the conjugate momentum to $\mathbf{A}(\mathbf{x}, t)$. It is worth pointing out that this is also the gauge where eqs. (1)-(3) naively make sense. As explained in [16, 18] eqs. (1)-(3) can be generalized to other gauges, but we will not need it here. We will study unequal-time correlators of the form

$$C_{12}(t) \equiv \frac{1}{V} \int d^3x \langle \mathcal{O}_1(\mathbf{x}, t) \mathcal{O}_2(\mathbf{x}, 0) \rangle, \quad (11)$$

where $\mathcal{O}_{1,2}$ are designed to probe the long-wavelength properties of interest. In particular, if one is interested in the magnetic degrees of freedom, a natural choice would be the autocorrelators of the magnetic field tensor and of its covariant curl:

$$\mathcal{O}_1(\mathbf{x}, t) = \mathcal{O}_2(\mathbf{x}, t) = \begin{cases} \mathbf{D} \times \mathbf{B}(\mathbf{x}, t) \\ \mathbf{B}(\mathbf{x}, t) \end{cases} \quad (12)$$

There is a special choice of $\mathcal{O}_{1,2}$ that allows to determine the color conductivity σ . Consider a correlator of $\mathbf{B}(\mathbf{x}, 0)$ with (6) at time t . It follows that

$$\sigma(t) \equiv \frac{\int d^3x \langle \mathbf{D} \times \mathbf{B}(\mathbf{x}, 0) \cdot \mathbf{D} \times \mathbf{B}(\mathbf{x}, t) \rangle}{\int d^3x \langle \mathbf{D} \times \mathbf{B}(\mathbf{x}, 0) \cdot \mathbf{E}(\mathbf{x}, t) \rangle} \longrightarrow \sigma, \quad (13)$$

if the time lag t is large compared to the autocorrelation time of the effective noise.

On the other hand, we can also study the autocorrelator of the color charge density

$$\rho \equiv \mathbf{D} \cdot \mathbf{E}, \quad (14)$$

if we are interested in detecting soft longitudinal excitations of the system (plasmons).

Note that all the space-local correlators of gauge-covariant quantities are invariant under the residual time independent gauge transformations which are not fixed by the choice of temporal gauge. However, if we transform these correlators away from the temporal gauge, they will in general depend on a Wilson line in the time direction, connecting $\mathbf{x}, 0$ to \mathbf{x}, t . This being the case, two remarks are in order. First, it is unclear to us to what extent (13) can serve as a genuine gauge invariant definition of color conductivity, since it is based on correlations between gauge covariant objects. In fact, as emphasized in [16] it is not very clear even in a perturbative framework how to define color conductivity beyond leading perturbative order. In [16] it was defined to next to leading order simply as the coefficient which appears in the effective theory (1)-(3), when formulated in temporal gauge or related, so called flow gauges, of which the Coulomb gauge is a limiting case. Our definition can be seen as an extrapolation of this philosophy: we have defined an effective theory by integrating out the high momentum part of the (classical) thermal theory and we then define σ by (1) and (2). Then a measurement of $\sigma(t)$ by (13) can be viewed as testing if our effective theory looks anything like (1) and (2).

Secondly, it is not a priori clear what effect the connecting temporal Wilson line has on the characteristic time scale of correlators between gauge-covariant quantities. For this reason, we also study the dynamics of a truly gauge-invariant object, $B^2(\mathbf{x}, x)$. As our results show, there is hardly any difference in correlation time scales for gauge-covariant and for gauge-invariant quantities.

3 Numerical results

A real-time correlator $C(t)$ of cooled classical gauge fields on a lattice depends on the following dimensional parameters: the temperature and the coupling constant in the unique combination g^2T , the system size L , the cooling time τ , and, finally, the lattice spacing a . As usual, we express all the other dimensional quantities in terms of the lattice spacing. The choice of other parameters is dictated by physical considerations. In particular, the inverse lattice temperature $\beta \equiv 4/(g^2Ta)$ is chosen within a range where the ratio of the perturbative Debye mass m_D to g^2T of the classical theory is close to that of the full SU(2) Yang-Mills theory at electroweak temperatures $T \sim 100\text{GeV}$. Since we are interested in the dynamics of fields with momenta of the order of g^2T , the dimensionless combination $L/(\beta a)$ should be large enough in order to avoid finite-size effects. Most of our simulations were performed at $L/(\beta a) = 2.4$. We verified that variations of $L/(\beta a)$ around that value did not

have a measurable effect. Finally, the cooling time τ should be large enough in order to suppress modes with momenta harder than those on the g^2T scale. In most our simulations $(g^2T)^2\tau = 3.84$. We saw that further increase of τ had little impact on the real-time behavior of the correlators.

Our original motivation for measuring real-time correlators of cooled fields was to determine the color conductivity, as explained in the previous section. We will discuss our (thus far unsuccessful) attempt to determine σ at the end of this section. However, the real-time correlators we measure are interesting in their own right, and we will first describe their properties as they transpired in the simulation.

In Figures 1 through 3 we present the autocorrelators $\langle \mathbf{D} \times \mathbf{B}(\mathbf{x}, t) \cdot \mathbf{D} \times \mathbf{B}(\mathbf{x}, 0) \rangle$, $\langle \mathbf{B}(\mathbf{x}, t) \cdot \mathbf{B}(\mathbf{x}, 0) \rangle$, and $\langle B_i^2(\mathbf{x}, t) B_i^2(\mathbf{x}, 0) \rangle - \langle B_i^2(\mathbf{x}, t) \rangle \langle B_i^2(\mathbf{x}, 0) \rangle$, respectively. Note that in the first two cases we determine autocorrelators of gauge-covariant quantities, whereas in the third case the quantity in question is gauge-invariant. In each case the autocorrelators are normalized by their value at the origin, while the time variable is expressed in units of $4/(g^2T)$. Notably, in all three cases the curves corresponding to different values of β coincide as long as the correlators retain a substantial fraction of their original value. This property is especially evident in the first two cases, where the error bars are smaller.

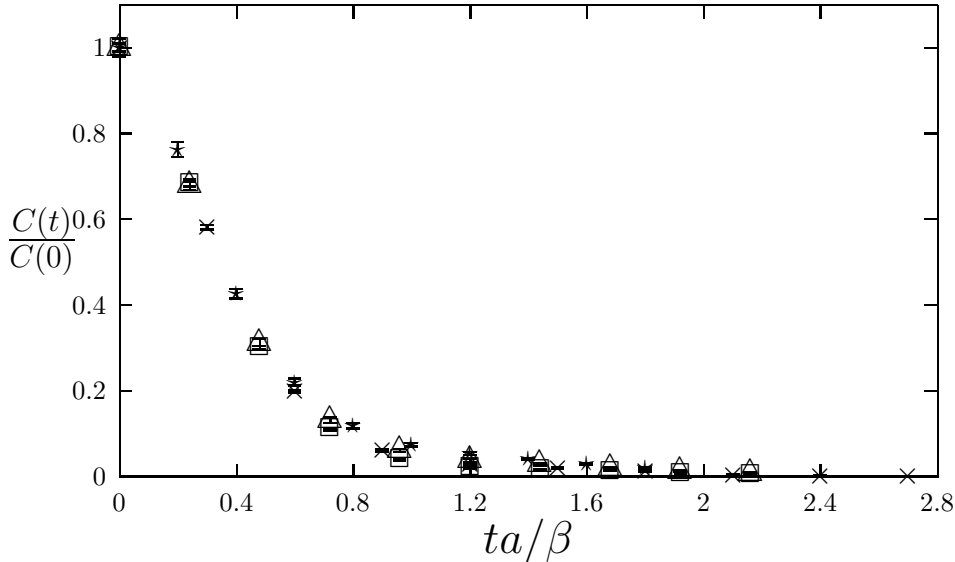


Figure 1: The autocorrelator $\langle \mathbf{D} \times \mathbf{B}(\mathbf{x}, t) \cdot \mathbf{D} \times \mathbf{B}(\mathbf{x}, 0) \rangle$ versus time t in units of $(g^2T)^{-1}$ for $\beta = 8.33$ (crosses), $\beta = 10.0$ (squares), $\beta = 12.5$ (triangles), and $\beta = 15.0$ (stars).

To further quantify this behavior of the time scales, we introduce the integral autocorrelation time defined for an autocorrelator $C(t)$ as

$$t_f \equiv (C(0))^{-1} \left(\int_0^\infty C(t) dt \right),$$

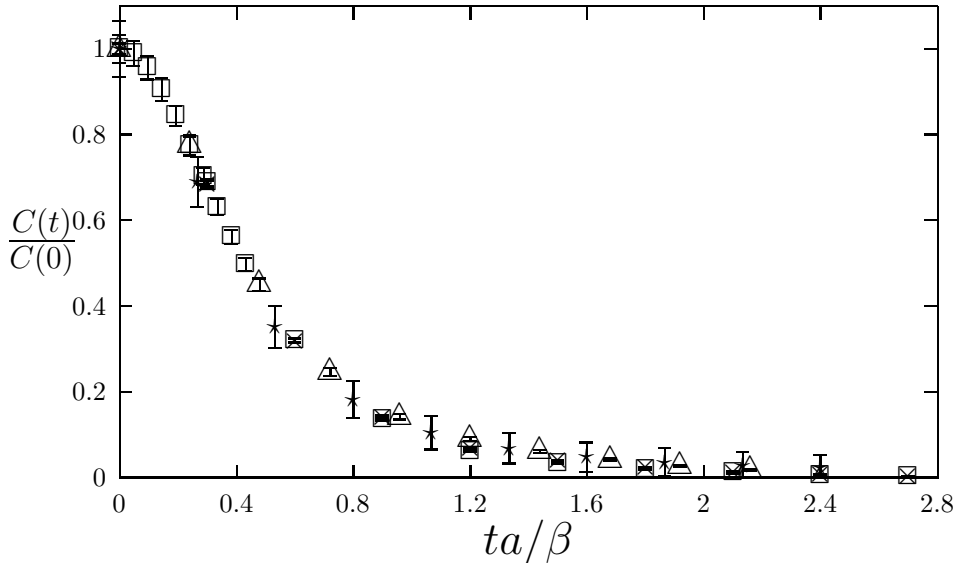


Figure 2: The autocorrelator $\langle \mathbf{B}(\mathbf{x}, t) \cdot \mathbf{B}(\mathbf{x}, 0) \rangle$ versus time t in units of $(g^2 T)^{-1}$ for $\beta = 8.33$ (crosses), $\beta = 10.0$ (squares), $\beta = 12.5$ (triangles), and $\beta = 15.0$ (stars).

where in our numerical estimates the upper limit of integration is replaced by a finite value t_u , for which $C(t_u)/C(0) \ll 1$. In Figure 4 we plot the dimensionless quantity $4/(g^2 T t_f)$ as a function of $1/\beta = g^2 T a/4$. Remarkably, in all three cases t_f turns out to be of the order of $g^2 T$ and shows little dependence on the lattice spacing throughout the range considered. There is therefore no evidence that in this range of the lattice spacings our cooled autocorrelators follow the ASY – Bödeker scenario, wherein the expected behavior is $t_f \propto 1/(g^4 T^2 a)$, up to logarithmic corrections.

The autocorrelator $\langle B_i^2(\mathbf{x}, t) B_i^2(\mathbf{x}, 0) \rangle$ turned out to be a much noisier quantity than the other two, resulting in much larger error bars despite comparable sample sizes in all the three cases. Apart from this difference, the integral autocorrelation times behave very similarly for the gauge-covariant and for the gauge-invariant quantities, even though the gauge-invariant autocorrelator of the former necessarily involves a straight adjoint Wilson line connecting the points \mathbf{x}, t and $\mathbf{x}, 0$.

Next, we consider the color charge autocorrelator $\langle \mathbf{D} \cdot \mathbf{E}(\mathbf{x}, t) \mathbf{D} \cdot \mathbf{E}(\mathbf{x}, 0) \rangle$. As shown in Figure 5, this quantity is strikingly different from the magnetic-field autocorrelators considered earlier. The time scale for the color charge correlation is proportional to the lattice spacing and does not depend on $g^2 T$.

This result can be contrasted with perturbative predictions. One would expect that the color-charge autocorrelator is dominated by the plasmon mode, whose frequency in the classical theory is of the order $g\sqrt{T/a}$ and whose decay rate is of the order $g^2 T$. We observe none of these properties in the range of lattice spacings considered.

Finally, we attempted to determine color conductivity σ , as defined in the In-

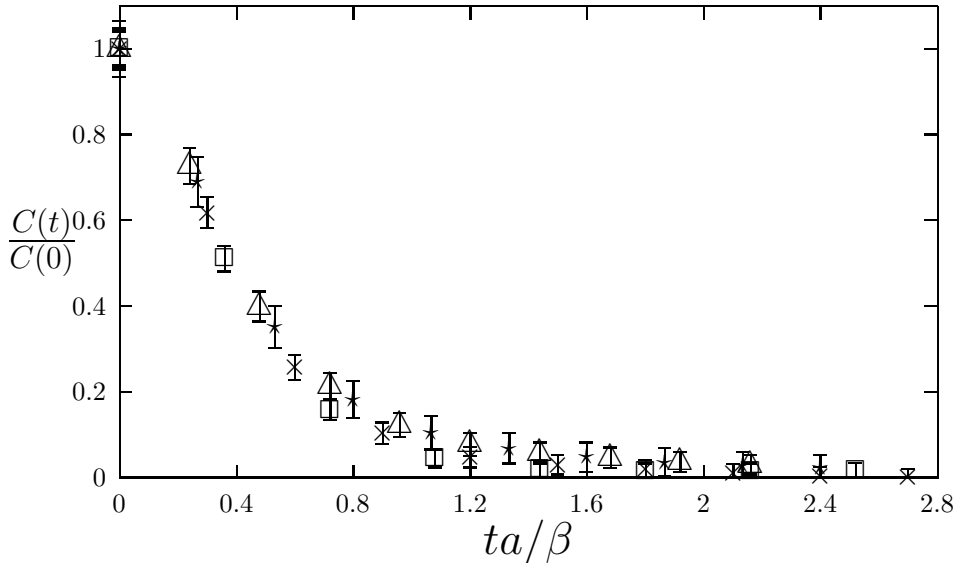


Figure 3: The connected autocorrelator $\langle B_i^2(\mathbf{x}, t)B_i^2(\mathbf{x}, 0) \rangle - \langle B_i^2(\mathbf{x}, t) \rangle \langle B_i^2(\mathbf{x}, 0) \rangle$ versus time t in units of $(g^2 T)^{-1}$ for $\beta = 8.33$ (crosses), $\beta = 10.0$ (squares), $\beta = 12.5$ (triangles), and $\beta = 15.0$ (stars).

roduction, using Eq. 13. As Figure 6 demonstrates, this attempt failed in two ways. First of all, $\sigma(t)$ does not appear to approach a constant for times in excess of the expected autocorrelation time of the noise term ξ (and far in excess of the measured autocorrelation time of the noise). Secondly, the numerical value of $\sigma(t)$ is very small (less than $0.25/a$) compared to the value expected in the ASY scenario ($a\sigma \approx 15$). Given this small value of $\sigma(t)$, it is not clear how neglecting the $\dot{\mathbf{E}}$ term in Eq. 1 can be justified.

4 Conclusion

In summary, we see no sign of the ASY-Bödeker scenario in the classical SU(2) theory, in the regime roughly corresponding to the electroweak scale. This negative finding does not rule out the ASY-Bödeker scenario in general, but one is led to question its applicability outside the asymptotically weak-coupling regime, which in the classical lattice theory corresponds to asymptotically small lattice spacing.

Neither our findings contradict earlier numerical data for the classical Yang-Mills theory, in particular, the sphaleron rate measurement by Moore and Rummukainen [7]. Their simulation was performed in the range of couplings (or lattice spacings) which overlaps the one considered here. Results of that work are consistent with the zero continuum limit of the rate, as predicted by ASY and by Bödeker. But they do not rule out a finite classical rate in the continuum.

This brings us to the following methodological remark. The sphaleron transition

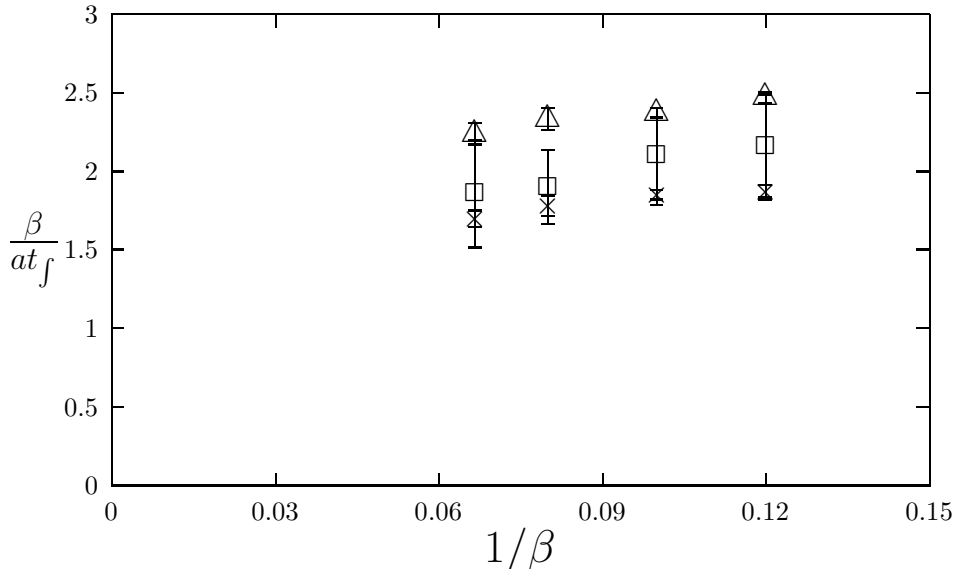


Figure 4: Inverse integral autocorrelation time in units of g^2T plotted against g^2Ta for $\langle \mathbf{D} \times \mathbf{B}(\mathbf{x}, t) \cdot \mathbf{D} \times \mathbf{B}(\mathbf{x}, 0) \rangle$ (triangles), $\langle \mathbf{B}(\mathbf{x}, t) \cdot \mathbf{B}(\mathbf{x}, 0) \rangle$ (crosses), and $\langle B_i^2(\mathbf{x}, t) B_i^2(\mathbf{x}, 0) \rangle - \langle B_i^2(\mathbf{x}, t) \rangle \langle B_i^2(\mathbf{x}, 0) \rangle$ (squares).

rate is a very important quantity in its own right, worthy of a careful numerical study. However, such study may not be the optimal way to test the theory of ASY and Bödeker. Precisely because the sphaleron rate is an essentially nonperturbative quantity, there is no easy way to disentangle the perturbative ASY-Bödeker damping from genuinely nonperturbative effects. To compound the difficulty, topology on a lattice is ill-defined and requires special treatment. By contrast, a study like the one reported here attempts to make a direct contact with perturbation theory, by measuring objects such as color conductivity. It therefore may be better suited for testing perturbative predictions.

Acknowledgement. The authors are grateful to P. Arnold, D. Bödeker, and L. Yaffe for illuminating discussions. The work of J.A. and K.N.A. was supported in part by “MaPhySto”, *Center of Mathematical Physics and Stochastics*—financed by the Danish National Research Foundation. J.A. and A.K. acknowledge the support of the Portuguese Fundação para a Ciência e a Tecnologia, under the research grants CERN/P/FIS/1203/98 and CERN/P/FIS/15196/1999. K.N.A.’s research was partially supported by the RTN grants HPRN-CT-2000-00122 and HPRN-CT-2000-00131 and a National Fellowship Foundation of Greece (IKY) postdoctoral fellowship. Finally, the authors acknowledge the support of the Danish Natural Science Council in making the simulations at the UNI-C computer center possible.

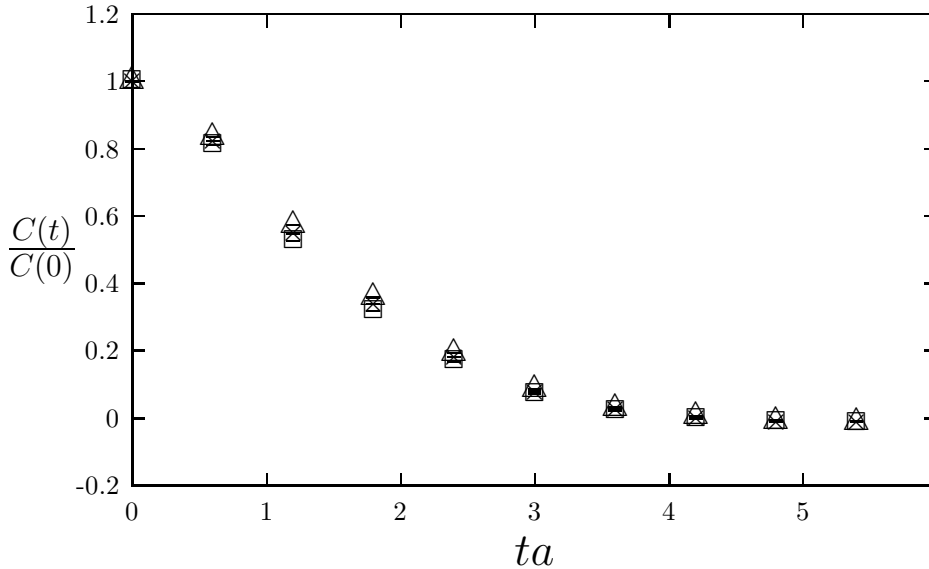


Figure 5: The autocorrelator $\langle \mathbf{D} \cdot \mathbf{E}(\mathbf{x}, t) \mathbf{D} \cdot \mathbf{E}(\mathbf{x}, 0) \rangle$ versus time t in lattice units for $\beta = 10$ (crosses), $\beta = 12.0$ (squares), and $\beta = 14.0$ (triangles) Note the complete or partial overlap of the data points.

References

- [1] V.A. Kuzmin, V.A. Rubakov and M.E. Shaposhnikov, Phys. Lett. **B155** (1985) 36.
- [2] Yu. Grigoriev, V.A. Rubakov and M.E. Shaposhnikov, Phys. Lett. **B216** (1989) 172.
- [3] J. Ambjørn, T. Askgaard, H. Porter and M.E. Shaposhnikov, Phys. Lett. **B244** (1990) 479; Nucl.Phys. **B353** (1991) 346.
- [4] J. Ambjørn and A. Krasnitz, Phys. Lett. **B362** (1995) 97, hep-ph/9508202.
- [5] A. Krasnitz, Nucl. Phys. **B455** (1995) 320, hep-lat/9507025.
- [6] D. Bödeker, Guy D. Moore and K. Rummukainen, Phys. Rev. **D61** (2000) 056003, hep-ph/9907545.
- [7] Guy D. Moore and Kari Rummukainen, Phys. Rev. **D61** (2000) 105008, hep-ph/9906259.
- [8] Guy D. Moore, Nucl. Phys **B568** (2000) 367, hep-ph/9810313; Phys. Lett. **B412** (1997) 359, hep-ph/9705248.
- [9] J. Ambjørn, A. Krasnitz, Nucl. Phys. **B506** (1997) 387, hep-ph/9705380.

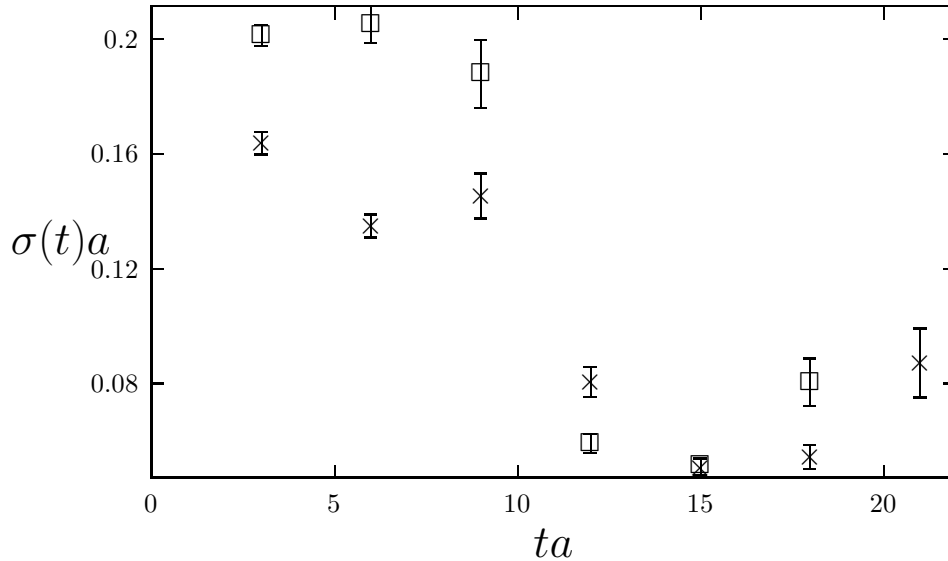


Figure 6: The color conductivity in lattice units defined as in Eq. 13 versus time t in lattice units for $\beta = 10$ (crosses) and $\beta = 12.0$ (squares).

- [10] Guy D. Moore, Chao-Ran Hu and Berndt Müller, Phys. Rev. **D58** (1998) 045001, hep-ph/9710436.
- [11] Guy D. Moore and Neil Turok, Phys. Rev. **D56** (1997) 6533, hep-ph/9703266; Phys. Rev. **D55** (1997) 6538, hep-ph/9608350.
- [12] M. Salle, J. Smit, J.C. Vink, *Scalar field dynamics: classical, quantum and in between*, hep-ph/0009120;
Gert Aarts and Jan Smit, Nucl. Phys. **B511** (1998) 451, hep-ph/9707342;
Wai-Hung Tang and Jan Smit, Nucl. Phys. **B510** (1998) 401, hep-lat/9702017;
Nucl. Phys. **B482** (1996) 265, hep-lat/9605016.
- [13] J. Ambjørn and K. Farakos, Phys. Lett. **B294** (1992) 248, hep-lat/9207020;
J. Ambjørn, K. Farakos, S. Hands, G. Koutsoumbas and G. Thorleifsson, Nucl. Phys. **B425** (1994) 39, hep-lat/9401028.
- [14] D. Bödeker, Phys. Lett. **B426** (1998) 351, hep-ph/9801430; Nucl. Phys. **B566** (2000) 402, hep-ph/9903478; Nucl. Phys. **B559** (1999) 502, hep-ph/9905239; *A local Langevin equation for slow long-distance modes of hot non-abelian gauge fields*, NBI-HE-00-46, hep-ph/0012304.
- [15] P. Arnold, D. Son, L. G. Yaffe, Phys. Rev. **D55** (1997) 6264, hep-ph/9609481; Phys. Rev. **D57** (1998) 1178, hep-ph/9709449; Phys. Rev. **D59** (1999) 105020, hep-ph/9810216.

- [16] P. Arnold, L. G. Yaffe, Phys. Rev. **D62** (2000) 125014, hep-ph/9912306; *ibid* 125013, hep-ph/9912305.
- [17] J. Ambjørn, M.L. Laursen and M.E. Shaposhnikov, Nucl. Phys. **B316** (1989) 483; Phys. Lett. **B197** (1987) 49.
- [18] P. Arnold, Phys. Rev. **E61** (2000) 6099, hep-ph/9912209.